Manuscript ID: 1184
DOI: 10.18462/iir.icr.2019.1184

Transcritical industrial heat pump using HFO's for up to 150°C hot air supply

Gisèle ABI CHAHLA[(1)], Yannick BEUCHER[(2)], Assaad ZOUGHAIB[(1)], Florence DE CARLAN[(2)], Jacques PIERUCCI[(3)]

[(1)] MINES ParisTech, PSL Research University, CES - Center for Energy efficiency of Systems, 5 rue Leon Blum, 91120 Palaiseau, France
assaad.zoughaib@mines-paristech.fr
[(2)] EDF Lab Les Renardières, Moret sur Loing et Orvanne, France
Florence.de-carlan@edf.fr
(3)R&D, Arjowiggins Graphic, Besse/Braye, France
jacques.pierucci@arjowiggins.com

ABSTRACT

Heat pumps may be used in drying processes to recover low-grade heat contained in moist exhaust air and supply the dryer. The heat pump design is limited technically by the level of process temperature and its performance optimization depends strongly on the difference between both temperature levels of process and effluents.
Using an exergy optimization methodology for heat pump integrations in industrial processes, a high temperature transcritical heat pump using the R-32 as working fluid was earlier proposed by the authors and experimentally demonstrated a 120°C hot air supply temperature.
In this paper, HFO's are considered to increase the air supply temperature to reach up to 150°C. Architecture technical options are also studied in order to improve the COP depending on the heat source and sink properties.
The prototype developed for the R-32 is adapted and used to validate the predicted performances. Its performance, when heating air from 90°C or 100°C to 150°C, is presented. The effluents are available at 82°C with different absolute humidities. The observed COP of the heat pump reached up to 3.72.
Keywords: Drying, Heat Recovery, HFO, Transcritical Cycle

1. INTRODUCTION

Due to the environmental concerns, improving energy efficiency of systems becomes a main challenge for all energy systems. This challenge implicates a better recovery of heat losses especially at high temperature in several industrial sectors. Indeed, a large amount of industrial sectors like paper drying needs heat at a high temperature range, typically 120°C-150°C, (Assaf 2010). In recent decades, studies dealt with the improvement of HPs energy efficiency especially those working at high temperature (Brown et al., 2009; Chamoun et al., 2012; Liu et al., 2012). Angelino (1994) demonstrated the advantages in an experimental point of view of the use of a transcritical HPs instead of subcritical HPs at high temperature for several stable fluids.
A thermodynamic model using Helmholtz multi-parametric equations to integrate the fluid properties was developed (Besbes et al., 2014) to predict the energy performances of transcritical HPs. And the results showed that 2 HFCs: R32, R134a and the HFO 1234yf have a great potential to maximize the energy efficiency of transcritical HPs at high temperature (120°C-130°C). This result led to a patent being registered (Peureux et al., 2014).
An experimental study dealing with the energy performance of a transcritical HP using the R32 as working fluid is presented by (Besbes et al., 2015). The operating conditions simulated a dryer

process. The heat source was humid air at 60°C (dew point at 45°C) and process air was heated from 60°C to 120°C. In this paper, the transcritical heat pump developed by Besbes et al. (2015) is adapted and used with the HFO 1234ze-E to increase the supply air temperature to 150°C.

2. EXPERIMENTAL METHODOLOGY

The experimental setup, designed in the previous work (Besbes et al., 2015), helped to demonstrate the high energy performance of a R32 transcritical HP. This experimental setup generates the conditions of an industrial dryer at the HP heat exchangers. Fig.1 provides the layout of a HP integrated with a preheater in a tunnel dryer. The effluents (moist air) preheat the ambient air moderately and get cooled to reach the saturation state. Then effluents pass through the evaporator to supply the HP with low grade heat. For this experimentation, only the HP energy performance was studied. The HP input operating conditions defined on the next paragraph were fixed with respect of the integration presented on Fig.1.

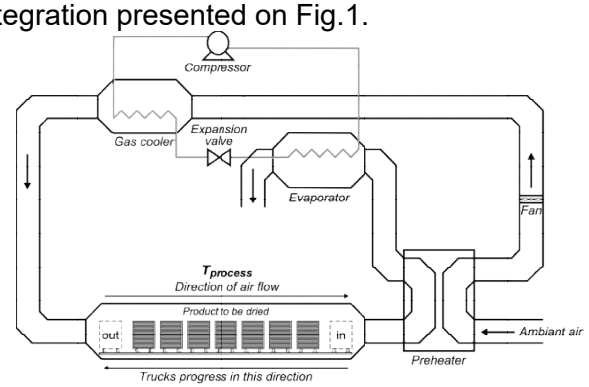

Figure 1:Schematic diagram of an integrated HP on a tunnel dryer process

2.1. Setup

To investigate the feasibility of delivering hot air at 150°C and the energy performance of the HFO1234ze-E transcritical HP system, the experimental setup is adapted and used. The main adaptation was the replacement of the lubricant. The fans were checked for their compatibility with higher temperature air. Moist air circulates on the cold loop. A schematic view of the experimental setup is shown in Fig. 2. The cold loop is composed of a steam humidifier, a fan, a heating resistor and valves to regulate the inlet evaporator air moisture content, temperature and mass flow rate. The hot loop is composed of a fan, a heating resistor, a valve system to control the temperature at the inlet of the gas cooler. Two sets of operating conditions are imposed on the test rig to try to get close to those of the typical drying processes (ADEME, 2006). For the first set (E1), the medium at the evaporator inlet is a humid air at 82°C with different level of absolute humidities ranging from 160 to 200 $gH_2O/kgDA$. The medium at the gas cooler inlet is an ambient air which was preheated from Tamb to 90°C to simulate the preheater of Fig.1, and the target temperature is fixed at 150°C.

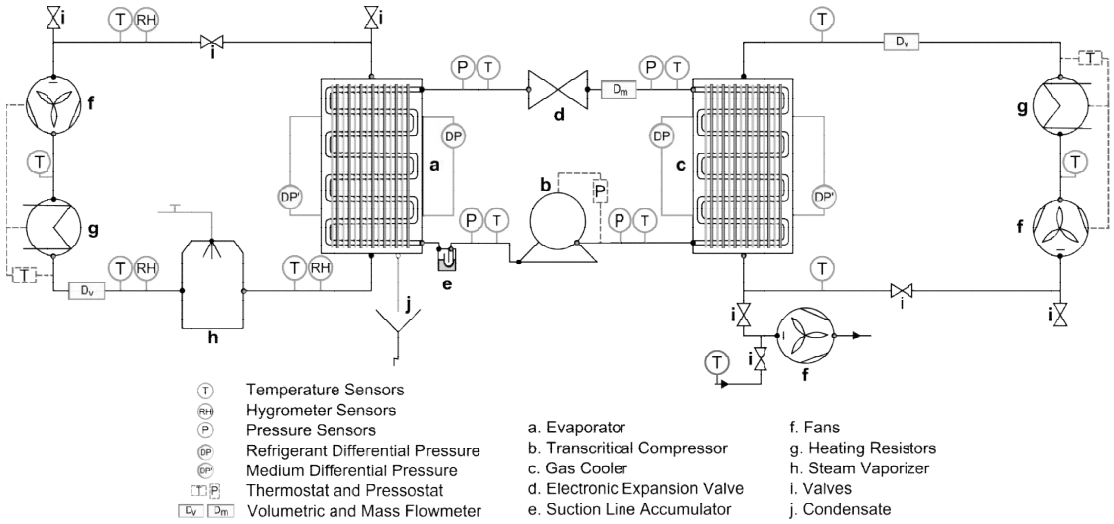

Figure 2: Test rig schematic view

For the second set (E2), the medium at the evaporator inlet is a humid air at 82°C with different level of absolute humidities ranging from 220 to 260 $gH_2O/kgDA$. The medium at the gas cooler inlet is an ambient air which was preheated from Tamb to 100°C, and the target temperature is fixed at 150°C.

The refrigerant loop is a single-stage vapour compression system. The following is a brief summary of the basic design and operating characteristics of the system:

- Refrigerant HFO1234ze-E was chosen as the working fluid of the heat pump (selected thanks to the methodology proposed in (Besbes et al, 2014). The critical temperature is equal to 109,4°C. And a polyolester synthetic oil (Reniso Triton se 170) was used as lubricant in the compressor.
- The gas cooler is an aluminium-finned stainless steel-tubes heat exchanger with dimensions of 0.30 m high x 0.60 m wide x 16 rows deep. The gas cooler has 1 circuit of 10 tubes per row of 12 mm external diameter and 2.5 mm pinch fins.
- The evaporator is an aluminium-finned stainless steel-tubes heat exchanger with dimensions of 0.72 m high x 0.75 m wide x 4 rows deep. The evaporator has 4 circuits of 6 tubes per row of 12 mm external diameter and 3 mm pinch fins.
- The compressor is a semi-hermetic reciprocating Bock HGX2/90 designed originally for R744 with a displacement of 7.70 m3/h at 50 Hz and a maximum discharge pressure of 13 000 kPa.
- A 3-phase induction motor is used to drive the compressor. The motor speed is controlled by a Danfoss, 3-phase, VLT HVAC frequency converter and the maximum input power of the motor is 11 kW.
- A CCM10 Danfoss electronic expansion valve designed for the R744 is used to control the refrigerant mass flow rate into the circuit and the gas superheat at the evaporator outlet.

Additional equipments of the heat pump included a suction line accumulator and compressor protection devices.

2.2. Instrumentation

The basic instrumentation required for evaluating the HP performance must include measurements of flow rate, temperatures, pressures and the electrical power input. Sensors were selected allowing defining the state conditions of the air and refrigerant at various localities shown in Fig.2. All the required readings were acquired at 10s intervals. Readings were considered for system performance analysis when they have been maintained steady for at least 20min.

Table 1 - List of measurement accuracies for the variables measured in the HP test rig

Measured property	Measuring sensors	Uncertainty on the value
Inlet and outlet refrigerant temperature	Class A RTD	±0.1 K
Inlet and outlet dry air temperature	Class A RTD	±0.1 K
Inlet and outlet air humidity	HC2-S ROTRONIC	±3% of measured value
Volume flow rate in the air loops	DEBIMO airfoil	±5%
Pressures in the air loops	CP300 KIMO	±0.5% + 1Pa
Pressures in the refrigerant circuit	PA21Y piezo resistive	±1%
Refrigerant mass flow rate	CORI FLOW	±0.2%
Compressor power input	3-Phase induction motor	±0.5%.

For the air loops, both dry and wet bulb temperature measurements were taken respectively at the gas cooler inlet and outlet and the evaporator inlet and outlet. The dry bulb temperatures were measured using stainless steel housing PT100 platinum resistance temperature devices (RTDs), and the wet bulb temperatures were measured by HC2-S ROTRONIC. At high relative humidity, the accuracy to measure the wet bulb temperature drops down. Thus, a lancing system was used to heat a moist air sample from the cold air loop. So the relative humidity decreases and the measure of the wet bulb temperature becomes more accurate. The volume flow rate was measured by the DEBIMO airfoil by KIMO for the two air loops. The differential pressures and pressures were measured by CP300 KIMO sensors. For the refrigerant circuit, temperatures and pressures were measured using respectively thermocouples and PA21Y piezo resistive pressure sensors, inserted through the walls of the refrigerant piping. As shown in Fig.2, locations of temperature and pressure sensors include the inlet and outlet of the compressor and gas cooler and the evaporator inlet. The refrigerant mass flow rate was measured by the CORI FLOW mass flow meter by BRONKHORST. The power input to the compressor was monitored using the Danfoss 3-phase induction motor and a wattmeter.

2.3. Experimental Tests

For all the tests performed in this work, the suction accumulator has been by passed to simplify the control. In our tests, the charge optimisation allows to reach the optimal high pressure. The expansion valve was controlled to maintain a reasonable super-heating value at the evaporator outlet, and simultaneously the motor speed compressor was controlled to reach the nominal point. The first tests served to determine the optimal refrigerant charge following the procedure proposed by Cho et al. (2005), Choi and Kim (2004) and Corberán et al. (2008). The optimal charge obtained for the first experimentations (7 kg) was kept for all the other operating conditions studied.
The tests series (E1) and (E2) were conducted at the full charge of the system under operating conditions introduced in previous paragraphs.

3. EXPERIMENTAL RESULTS AND DISCUSSION

Tests are performed using the experimental setup described earlier. The two experimentations set conditions are applied and for all the tests, the air exiting the gaz cooler attained 150°C. This temperature was controlled by adjusting the compressor rotating speed and the air flow rate. The control of the expansion valve insured a superheating of 5K for all the tests.
Table 2 gives the experimental results for both sets.
Results in table 2 show that the absolute humidity impacts directly the evaporator pressure.
Fig.3 shows the measured COP of the heat pump for each test. The COP is determined with an uncertainty of +/-3.3%.
The COP of the heat pump increases with the absolute humidity which is a direct consequence of the evaporating pressure increase. It is also noticed that the COP of the set E1 is higher than the COP of the set E2 even though the evaporator pressure is lower in set E1 than the one obtained in E2

Table 2 – Experimental results for the 2 experimentations sets (E1)and (E2)

		E1			E2		
Absolute humidity of input air temperature at the evaporator	g_{H2O}/kg_{DA}	160	180	200	220	240	260
Input air temperature at the evaporator	°C	82	82	82	82	82	82
Dew point of input air at the evaporator	*°C*	60.9	62.8	65.1	66.6	68.0	69.2
Input air temperature at the gas cooler	°C	90	90	90	100	100	100
Gaz cooler air outlet Temperature	°C	150	150	150	150	150	150
Gaz cooler pressure	*bar*	68.2	67.5	67.1	67.0	66.3	68.2
Evaporator pressure	*bar*	12.4	13	13.5	13.9	14.1	15.1
Evaporator capacity	*kW*	8.10	7.66	8.01	7.08	7.74	8.32
Gas cooler capacity	*kW*	11.34	10.54	11.15	10.13	11.01	11.79
Compressor power	*kW*	3.24	2.88	2.99	3.05	3.27	3.47

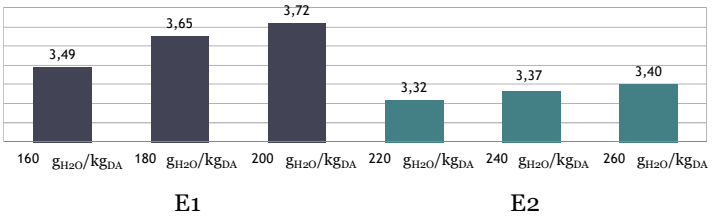

Figure 3: COP values for both sets (E1) and (E2)

Fig. 4 shows the evolution of vapor quality at the evaporator inlet for the realized tests.
The vapour quality at the inlet of the evaporator is significantly lower for the set E1 than the set E2. This is due mainly to the hot air inlet temperature (90°C for the set E1 and 100°C for the set E2) which impacts the refrigerant temperature at the outlet of the gaz cooler and hence the enthalpy at the inlet of the evaporator.

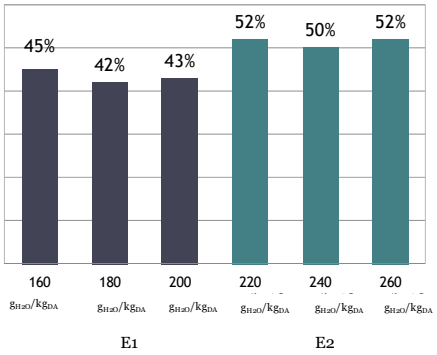

Figure 4 – Vapor quality at the inlet of the evaporator (in %)

Figure 5 shows on a T-H diagram how the change in the air inlet temperature impacts the cycle.

Indeed, as we can see in Fig. 5, the dashed part of the cycle is obtained for lower gaz cooler exit temperature. This temperature is directly impacted by the hot air inlet temperature. The resulting consequence is a lower vapour quality at the inlet of the evaporator and so a larger enthalpy change leading to an increased capacity at the evaporator for the same compression cost; which

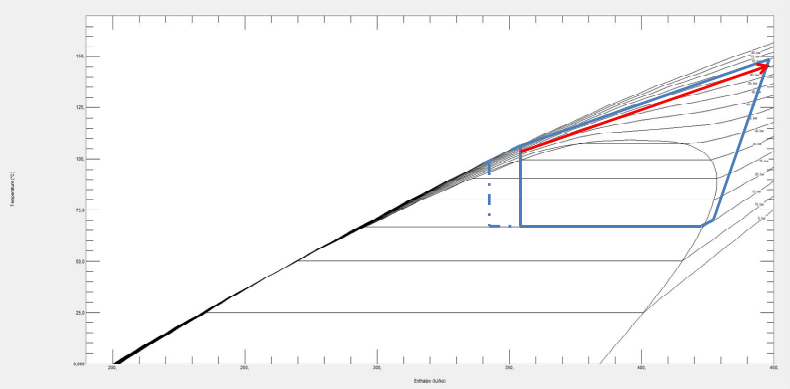

Figure 5: Effect of hot air inlet temperature on the cycle

explains the COP increase observed during the tests. This observation allows proposing technical options for improving the COP of such a heat pump using R-1234ze and supplying hot air at 150°C.

4. TECHNICAL OPTIONS FOR IMPROVING THE CYCLE

The experimental results presented in section 3 and their analysis have shown that the refrigerant temperature at the outlet of the gaz cooler will have a very important impact on the heat pump's COP. In the prototype, this temperature is directly linked to the hot air inlet temperature as it was highlighted between test sets E1 and E2.

One technical option, when the refrigerant properties are favourable, is to use an internal heat exchanger. Such a heat exchanger allows reducing the gaz cooler outlet temperature while increasing the superheat at the inlet of the compressor. Another technical option, which was studied for CO2 transcritical refrigeration cycles, is to use a parallel compression (Sarkar and Agrawal, 2010). Such a compression allows vapour compression on a smaller pressure difference reducing the main compressor input power.

Figures 6 and 7 show, in a T-H diagram, the simplified cycle including respectively the internal heat exchanger and the parallel compression.

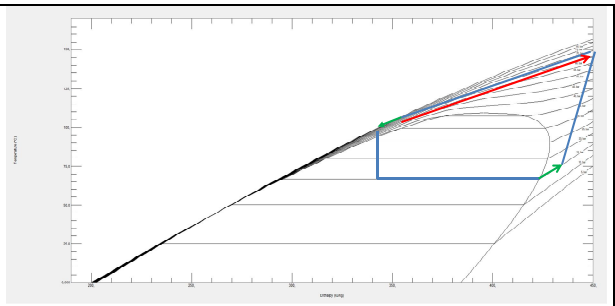

Figure 6 – T-H diagram of simplified transcritical cycle with IHX

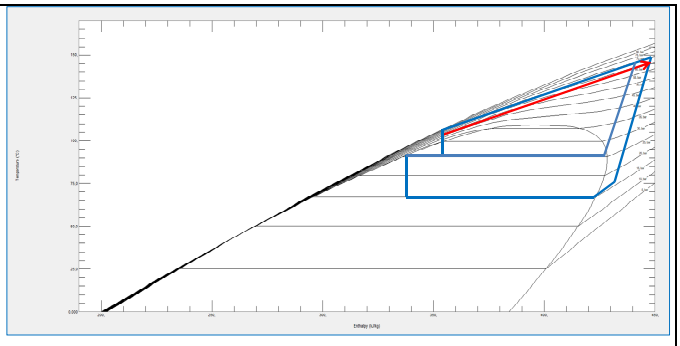

Figure 7 - T-H diagram of simplified transcritical cycle with parallel compression

These technical options where simulated for the first test of the E2 set (Evaporator air inlet temperature 82°C, absolute humidity 220 g/Kg_{da}, gaz cooler inlet air temperature 100°C). The simulation code is written in Python using Coolprop for the calculation of refrigerant properties. The main equations are first and second law and mass conservation. First the internal heat exchanger (IHX) was investigated, then the parallel compression and finally, combining both options.

The COP improvement is given in table 3.

Table 3 – COP improvement with IHX and parallel compression

Cycle	Transcritical	Transcritical+IHX	Transcritical+parallel compression	All options
COP	3.32	3.51	3.61	3.71

As we can see in table 3, parallel compression allows a 9% COP improvement. The use of IHX allows 6% COP improvement. The combination of the two options, by subcooling the liquid exiting the gaz cooler just before the first expansion, allows an improvement of 12% of the COP.
Indeed, both options allow the reduction of the evaporator inlet quality. This helps reducing the expansion valve losses. The parallel compression has an additional advantage of reducing the refrigerant mass flow to be compressed by the main compressor while compressing the rest of the mass flow at a lower pressure ratio.

5. CONCLUSIONS

The following conclusions can be drawn from the present analysis. The transcritical HP using the HFC 32 developped earlier has been able to supply 150°C hot air temperature by changing its working fluid to HFO-1234ze-E. The COP of the transcritical HP was measured for several operating conditions. In the worst operating conditions the HP presents a COP equal to 3.32 while it reached 3.72 for the most favourable ones. For the transcritical cycle, the vapor quality at the evaporator inlet is impacted by the conditions at the gaz cooler exit ones and affects the COP. Two technical options for improving the COP were simulated. They allow an improvement of 12% of the COP.

6. AKNOWLEDGEMENTS

The authors would like to aknowledge the financial support of ADEME through the TRANSPAC AMI project

7. REFERENCES

Angelino, G. Invernizzi, C., Supercritical heat pump cycles, International Journal of Refrigeration, Volume 17, Issue 8, 1994, Pages 543-554, ISSN 0140-7007.

Assaf, Khattar. 2010. Intégration D'une Pompe À Chaleur Dans Un Procédé Agroalimentaire - Simulation, Expérimentation et Intégration. Ph.D thesis, École Nationale Supérieure des Mines de Paris.

Besbes, Karim, Assaad Zoughaib, Florence De Carlan, and Jean-Louis Peureux. 2014. Exergy Based Methodology for Optimized Integration of Heat Pumps in Industrial Processes. International Refrigeration and Air Conditioning Conference at Purdue. http://docs.lib.purdue.edu/iracc/1435.

Besbes, Karim, Assaad Zoughaib, Florence De Carlan, and Jean-Louis Peureux. 2015. A R-32 TRANSCRITICAL HEAT PUMP FOR HIGH TEMPERATURE INDUSTRIAL APPLICATIONS. International Congress of Refrigeration, Yokohama.

Brown, J. Steven, Claudio Zilio, and Alberto Cavallini. 2009. The Fluorinated Olefin R-1234ze(Z) as a High-Temperature Heat Pumping Refrigerant. International Journal of Refrigeration 32(6): 1412–22. http://www.sciencedirect.com/science/article/pii/S0140700709000772 (February 14, 2014).

Chamoun, Marwan, Romuald Rulliere, Philippe Haberschill, and Jean Francois Berail. 2012. Dynamic Model of an Industrial Heat Pump Using Water as Refrigerant. International Journal of

Refrigeration 35(4): 1080–91.
http://www.sciencedirect.com/science/article/pii/S0140700711003082.

Cho, Honghyun, Changgi Ryu, Yongchan Kim, and Ho Young Kim. 2005. Effects of Refrigerant Charge Amount on the Performance of a Transcritical CO2 Heat Pump. International Journal of Refrigeration 28(8): 1266–73.

Choi, Jongmin, and Yongchan Kim. 2004. Influence of the Expansion Device on the Performance of a Heat Pump Using R407C under a Range of Charging Conditions. International Journal of Refrigeration 27: 378–84.

Corberán, Jose M., Israel O. Martínez, and José Gonzálvez. 2008. Charge Optimisation Study of a Reversible Water-to-Water Propane Heat Pump. International Journal of Refrigeration 31(4): 716–26. http://www.sciencedirect.com/science/article/pii/S0140700707002484 (December 12, 2014).

ADEME : Le sechage thermique. Rapport technique, ADEME, Département Industrie et Agriculture, 2006.

Liu, Zhaoyong, Li Zhao, Xuezheng Zhao, and Hailong Li. 2012. The Occurrence of Pinch Point and Its Effects on the Performance of High Temperature Heat Pump. Applied Energy 97: 869–75.

Meunier, Francis, Paul Rivet, and Marie-france Terrier. Froid Industriel 2ed.

Peureux, Bourig, Zoughaib, Besbes. Equipement including a heat pump for heating an external fluid with a large temperature differential. International Patent WO2014020255 (A1), 2014.

Sarkar J.,Agrawal N. Performance optimization of transcritical CO2 cycle with parallel compression economization. International Journal of Thermal Sciences. Volume 49, Issue 5, May 2010, Pages 838-843

Zhao, Chen Ru, and Pei Xue Jiang. 2011. Experimental Study of in-Tube Cooling Heat Transfer and Pressure Drop Characteristics of R134a at Supercritical Pressures. Experimental Thermal and Fluid Science 35(7): 1293–1303.